



## OPEN ACCESS

## EDITED BY

Paola Marziani,  
Osservatorio Astronomico di Padova  
(INAF), Italy

## REVIEWED BY

Andjelka Branislav Kovacevic,  
University of Belgrade, Serbia  
Marko Stalevski,  
Astronomical Observatory, Serbia  
Elena Shablovinskaya,  
Diego Portales University, Chile

## \*CORRESPONDENCE

Hermine Landt,  
✉ hermine.landt@durham.ac.uk

RECEIVED 10 July 2023

ACCEPTED 05 September 2023

PUBLISHED 25 September 2023

## CITATION

Landt H (2023), The outer dusty edge of  
accretion disks in active galactic nuclei.  
*Front. Astron. Space Sci.* 10:1256088.  
doi: 10.3389/fspas.2023.1256088

## COPYRIGHT

© 2023 Landt. This is an open-access  
article distributed under the terms of the  
[Creative Commons Attribution License  
\(CC BY\)](https://creativecommons.org/licenses/by/4.0/). The use, distribution or  
reproduction in other forums is  
permitted, provided the original author(s)  
and the copyright owner(s) are credited  
and that the original publication in this  
journal is cited, in accordance with  
accepted academic practice. No use,  
distribution or reproduction is permitted  
which does not comply with these terms.

# The outer dusty edge of accretion disks in active galactic nuclei

Hermine Landt\*

Department of Physics, Centre for Extragalactic Astronomy, Durham University, Durham, United Kingdom

Recent models for the inner structure of active galactic nuclei (AGN) aim at connecting the outer region of the accretion disk with the broad-line region and dusty torus through a radiatively accelerated, dusty outflow. Such an outflow not only requires the outer disk to be dusty and thus predicts disk sizes beyond the self-gravity limit but requires the presence of nuclear dust with favorable properties. Here, we investigate a large sample of type 1 AGN by near-infrared (near-IR) cross-dispersed spectroscopy with the aim to constrain the astrochemistry, location, and geometry of the nuclear hot dust region. Assuming a thermal equilibrium for optically thin dust, we derive the luminosity-based dust radius for different grain properties using our measurement of the temperature. We combine our results with independent dust radius measurements from reverberation mapping and interferometry, and show that large dust grains that can provide the necessary opacity for the outflow are ubiquitous in AGN. Using our estimates of the dust covering factor, we investigate the dust geometry using the effects of the accretion disk anisotropy. A flared disk-like structure for the hot dust is favored. Finally, we discuss the implication of our results for the dust radius-luminosity plane.

## KEYWORDS

active galactic nuclei, quasars, dust continuum emission, dust physics, near-infrared astronomy

## 1 Introduction

A prominent feature in the multi-wavelength spectral energy distributions (SEDs) of active galactic nuclei (AGN) is strong infrared (IR) continuum emission, which originates from thermal dust radiation. The structure of the dust producing it is commonly assumed to be an optically thick toroid, which is aligned with the plane of the accretion disk. The accretion disk then provides the UV/optical photons that heat the dust. An alternative to the dusty torus was already proposed previously by [Phinney \(1989\)](#), namely, an extended and warped dusty disk. Such a structure is attractive since it could present a natural transition between the accretion disk and the central dust, without the stability problem of the torus ([Krolik, 2007](#)).

The extended dust structure emits over a large IR wavelength range, with the near-IR believed to be dominated by the hottest dust located closest to the central supermassive black hole. Therefore, AGN are most suitable to investigate the chemical composition and grain properties of astrophysical dust. Their UV/optical luminosities are usually high enough to heat the central dust to sublimation temperatures, a property which they have in common with protoplanetary disks around young stars. If we can observe these high temperatures,

we can, in principle, constrain the chemistry since different species condense out of the gas phase in different environmental conditions. Previously, dust temperatures were measured in a handful of AGN by obtaining simultaneous photometry at several near-IR wavelengths (Clavel et al., 1989; Glass, 2004; Schnülle et al., 2013; 2015) but has only come of age with the availability of efficient near-IR cross-dispersed spectrographs. Landt et al. (2011b) and Landt et al. (2014) derived dust temperatures from such spectroscopy for the largest sample of type 1 AGN so far ( $\sim 30$  sources). They found a very narrow dust temperature distribution with an average value of  $T \sim 1400$  K. This result, which is similar to what has been found in protoplanetary disks (Monnier et al., 2005), either indicates dust at sublimation but composed mainly of silicate grains and so an oxygen-rich environment from which the dust formed, or if carbon dominates the composition, then the dust is *not* heated close to sublimation since carbonaceous dust, e.g., graphite, can survive up to  $T \sim 2000$  K (Salpeter, 1977).

The first near-IR *spectroscopic* monitoring campaign of the hot dust in an AGN, namely, NGC 5548, found that a single component dominated both the mean and variable emission, with the dust response time and luminosity-based dust radius being consistent with each other if the emissivity of a pure blackbody was assumed (Landt et al., 2019). Thus, the dust grain size of the hot dust in this AGN could be constrained to relatively large values (of a few  $\mu\text{m}$ ). From the estimated dust temperature and its variability, they concluded that the dust composition was predominantly carbonaceous and well below the sublimation threshold. The reverberation signal of the dust was then mainly due to a heating and cooling process in response to the variable UV/optical accretion disk flux irradiating it. Most importantly, the dust reverberation signal showed tentative evidence for a second hot dust component most likely associated with the accretion disk. The existence of dust in the outer regions of the accretion disk is a prerequisite for the recent models of the AGN structure proposed by Czerny et al. (2017) and Baskin and Laor (2018). These authors explain both the broad emission line region (BLR) and the dusty torus as part of the same outflow launched from the outer accretion disk by radiation pressure on dust. Since carbonaceous dust has a higher opacity than silicate dust, the former is preferred in this scenario. Most recently, Landt et al. (2023) presented results from a near-IR spectroscopic monitoring campaign on the high-luminosity AGN Mrk 876. The comparison of the mean and variable (rms) spectra clearly showed that at least two hot dust components are present in AGN, with the second component possibly originating in the accretion disk. However, contrary to the case of NGC 5548, the independent measure of the dust radius via reverberation mapping yielded a value a factor of  $\sim 2$  lower than the luminosity-based dust radius estimate, indicating that the anisotropy effects of the accretion disk illumination and through it the dust geometry can be detected and studied in this way. For Mrk 876, it was concluded that the geometry is most likely a flared, dusty disk with an enlarged ‘inner hole,’ which is very similar to the paradigm commonly assumed for protoplanetary disks.

Given the high potential that a comparison between luminosity-based dust radii and those obtained by independent methods, e.g., by reverberation mapping, carries for revealing the astrochemistry and geometry of the hot dust in AGN, this study sets out to apply it to a large sample of AGN. In Section 2, we discuss the selection

of the sample, whereas Section 3 gives details of the measurements required for the estimation of the luminosity-based dust radius. In Section 4, we discuss our main results and finally present the conclusion in Section 5.

## 2 Sample selection

As discussed by Landt et al. (2019, 2023), combining the assumption of a radiative equilibrium of optically thin dust, which encodes a dependence on the dust chemical species and grain size through the dust emissivity parameter (see Eq. 1), with an independent measurement of the dust radius can constrain the dust astrochemistry. Alternative dust radius measurements can be determined, e.g., the dust response time estimated by reverberation mapping or the geometric distance of the dust measured through near-IR interferometry. A promising new method is also the estimate of the location of the scattering region through optical spectropolarimetry of the BLR (Shablovinskaya et al., 2020). Therefore, this study required a sample of type 1 AGN with an optical/near-IR continuum dominated by AGN rather than the host galaxy starlight. Furthermore, the available near-IR spectrum should cover a sufficiently large wavelength range to allow for both an estimate of the accretion disk flux level and a measurement of the hot dust temperature in order to be able to calculate the luminosity-based dust radius. This requirement is usually met only by cross-dispersed near-IR spectra (Landt et al., 2011b). Finally, the type 1 AGN with available cross-dispersed near-IR spectra were required to have a published near-IR dust radius based on an alternative method. The total sample comprises 39 objects, and its properties are listed in Table 1. The independent dust radius measurement was mostly from near-IR (photometric) dust reverberation mapping campaigns covering the wavelength region of up to a few  $\mu\text{m}$  and, thus, sampling the SED of the hot dust, and in only 4/39 sources, the dust radius measurement was based on near-IR interferometry.

## 3 Luminosity-based dust radius

The calculation of the luminosity-based dust radius requires a measurement of the dust temperature and an estimate of the UV/optical (accretion disk) luminosity that heats the dust. Cross-dispersed near-IR spectra with their relatively large wavelength range cover about half the hot dust SED in low-redshift AGN and additionally a considerable part of the accretion disk spectrum. The latter is expected to be the dominant contributor to the continuum flux up to  $\sim 1 \mu\text{m}$  (Landt et al., 2011a; b). In order to obtain the necessary measurements, we decomposed the spectral continuum into these two components, accretion disk and dust emission, following the approach described in Landt et al. (2019). As already noted in Landt et al. (2019), due to the relatively small spectral aperture usually used for near-IR spectroscopy, the contribution of host galaxy light to the total observed continuum flux is expected to be negligible in most AGN. In short, we have first approximated the rest-frame wavelength range of  $\lesssim 1 \mu\text{m}$  with the spectrum of a standard accretion disk, which we have subsequently subtracted from the total spectrum. For the calculation of the accretion

TABLE 1 Sample.

Object name	$z$	$\text{Log } L_{\text{UV}}$ ( $\text{erg s}^{-1}$ )	$T_{\text{d}}$ (K)	$\text{Log } L_{\text{d}}$ ( $\text{erg s}^{-1}$ )	$R_{\text{d,lum}}$ (lt days)	Reference	$R_{\text{d,rev}}$ (lt days)	Reference
(1)	(2)	(3)	(4)	(5)	(6)	(7)	(8)	(9)
3C 351	0.372	46.63	1,373	46.78	792	R06	$1,203 \pm 542$	Lyu19
PG 2233 + 134	0.326	46.85	1,413	45.65	964	This work	$343 \pm 29$	Lyu19
PG 0953 + 414	0.234	46.45	1,391	45.75	627	This work	$566^{+50}_{-38}$	M19
PG 0947 + 396	0.206	45.22	1,406	44.96	149	This work	$1,629 \pm 23$	Lyu19
PDS 456	0.184	47.41	1,425	46.83	1806	L08	$1,599 \pm 213^*$	G20
3C 273	0.158	47.59	1,443	46.76	2,166	L08	$1,656 \pm 59$	Lyu19
PG 0052 + 251	0.155	46.07	1,198	45.29	546	L13	$347 \pm 37$	Lyu19
PG 1307 + 085	0.155	46.22	1,307	45.25	545	L13	$310 \pm 40$	Lyu19
PG 0026 + 129	0.145	46.41	1,127	45.15	913	L13	$487 \pm 36$	Lyu19
PG 1519 + 226	0.137	45.85	1,538	45.24	257	R06	$170 \pm 99$	Lyu19
PG 1612 + 261	0.131	45.67	1,549	45.25	206	R06	$555 \pm 35$	Lyu19
Mrk 876	0.129	46.09	1,306	45.55	469	L23	$334^{+42}_{-37}$	M19
PG 1415 + 451	0.114	45.92	1,461	45.07	309	R06	$269 \pm 208$	Lyu19
PG 0804 + 761	0.100	45.97	1,314	45.70	405	L13	$600 \pm 21$	Lyu19
PG 1211 + 143	0.081	46.22	1,337	45.10	521	L13	$338 \pm 83$	Lyu19
Mrk 478	0.079	46.11	1,547	45.34	343	R06	$237 \pm 37$	Lyu19
PG 1448 + 273	0.065	45.31	1,477	44.55	150	R06	$263 \pm 30$	Lyu19
PG 0844 + 349	0.064	46.18	1,190	44.76	628	L11	$99^{+13}_{-10}$	M19
Mrk 1,513	0.063	46.33	1,356	45.04	575	L13	$494 \pm 42$	Lyu19
I Zw 1	0.060	45.58	1,412	45.21	224	G12	$274 \pm 41$	Lyu19
PG 1126–041	0.060	45.65	1,515	45.09	211	R06	$523 \pm 26$	Lyu19
Mrk 734	0.050	45.70	1,597	44.48	201	This work	$103 \pm 7$	Lyu19
Mrk 231	0.041	45.67	1,529	45.71	212	This work	$393 \pm 83^*$	K09
Mrk 841	0.036	45.22	1,437	44.23	143	P22	$110 \pm 15$	Lyu19
Mrk 110	0.035	46.00	1,452	44.56	343	L11	$117 \pm 6$	K14
Mrk 509	0.034	45.77	1,398	44.79	284	L08	$121 \pm 2$	K14
Ark 120	0.033	45.45	1,102	45.16	316	L08	$138 \pm 18$	K14
3C 120	0.033	45.28	1,389	44.59	164	L13	$94^{+4}_{-7}$	R18
Mrk 817	0.031	45.65	1,401	44.53	246	L11	$93 \pm 9$	K14
Mrk 290	0.030	45.36	1,353	44.26	189	L08	$124 \pm 3$	Lyu19
H 2106–099	0.027	45.28	1,342	44.27	175	L08	$303 \pm 36^*$	G23
Mrk 335	0.026	45.63	1,308	44.40	276	L08	$168 \pm 6$	K14
Mrk 79	0.022	44.82	1,364	44.21	100	L11	$68 \pm 5$	K14
Mrk 1,239	0.019	44.85	1,443	44.64	92	R06	$189 \pm 30^*$	G23
NGC 5548	0.017	44.50	1,450	44.02	61	L19	$75 \pm 8$	L19
NGC 7469	0.016	45.28	1,551	44.19	131	L08	$85 \pm 1$	K14

(Continued on the following page)

TABLE 1 (Continued) Sample.

Object name	$z$	$\text{Log } L_{\text{uv}}$ ( $\text{erg s}^{-1}$ )	$T_d$ (K)	$\text{Log } L_d$ ( $\text{erg s}^{-1}$ )	$R_{d,\text{lum}}$ (lt days)	Reference	$R_{d,\text{rev}}$ (lt days)	Reference
(1)	(2)	(3)	(4)	(5)	(6)	(7)	(8)	(9)
NGC 3783	0.010	45.23	1,472	44.01	138	P22	$131^{+25}_{-30}$	E23
NGC 4593	0.009	44.72	1,380	43.71	87	L08	$42 \pm 1$	K14
NGC 4151	0.003	43.24	1,328	43.06	17	L08	$46 \pm 1$	K14

The columns are: (1) object name; (2) redshift; (3) total accretion disk luminosity for a blackbody emissivity; (4) dust temperature; (5) total dust luminosity; (6) dust radius; (7) reference for the cross-dispersed near-IR, spectral data used for the continuum fits; and (8) near-IR, dust reverberation lag time in the rest-frame taken from reference in (9). References are E23: Esser et al. (2023), G12: Garcia-Rissmann et al. (2012), G20: Dexter et al. (2020), G23: Amorim et al. (2023), K09: Kishimoto et al. (2009), K14: Koshida et al. (2014), L08: Landt et al. (2008), L11: Landt et al. (2011b), L13: Landt et al. (2013), L19: Landt et al. (2019), L23: Landt et al. (2023), Lyu19: Lyu et al. (2019), M19: Minezaki et al. (2019), P22: Prieto et al. (2022), R06: Riffel et al. (2006), and R18: Ramolla et al. (2018).

\* near-IR, interferometric dust radius.

disk spectrum, we adopted the black hole mass listed in Bentz and Katz (2015) for a geometrical scaling factor of  $f=4.3$ , where available, and else, we have estimated it based on the relationship between black hole mass and near-IR virial product presented in Landt et al. (2013). The scaling of the accretion disk spectrum to the near-IR spectrum then readily gives the accretion rate. Furthermore, we assumed that the disk is relatively large and extends out to  $r_{\text{out}} = 10^4 r_g$ . We then fitted the resultant hot dust spectrum at wavelengths  $>1 \mu\text{m}$  with a blackbody, representing emission by large dust grains. Table 1 lists the physical parameters derived from the near-IR spectral decomposition. As shown in Landt et al. (2019), we then calculated luminosity-based dust radii,  $R_{d,\text{lum}}$ , from the best-fit dust temperatures assuming radiative equilibrium between the luminosity of the irradiating source and the dust:

$$\frac{L_{\text{uv}}}{4\pi R_{d,\text{lum}}^2} = 4\sigma T^4 \langle Q^{\text{em}} \rangle, \quad (1)$$

where  $\sigma$  is the Stefan–Boltzmann constant and  $\langle Q^{\text{em}} \rangle$  is the Planck-averaged emission efficiency. We have approximated  $L_{\text{uv}}$  with the accretion disk luminosity, as given in Table 1, and have used  $\langle Q^{\text{em}} \rangle = 1$ , which is appropriate for the case of a blackbody. The blackbody case is reached for grain sizes of  $a \geq 0.4 \mu\text{m}$  and  $\geq 2 \mu\text{m}$  for carbon and silicate dust, respectively (see Fig. 8 of Landt et al., 2019). As Landt et al. (2019, 2023) have shown, radii for dust composed of small grains ( $a \leq 0.1 \mu\text{m}$ ) are a factor of  $\sim 6$  and  $\sim 10$  larger if the composition is mainly carbonaceous or silicates, respectively. The error on the luminosity-based dust radius is determined by the error on the temperature and the error on the total accretion disk luminosity. Due to the relatively large wavelength coverage of the cross-dispersed near-IR spectra, which are also of relatively high signal-to-noise, the error on the temperature is small ( $\sim 10 - 30$  K; Landt et al., 2019; 2023). The accretion disk luminosity is mostly determined by the accretion rate, which is set by the flux level of the near-IR spectrum. As discussed in Landt et al. (2019, 2023), since the telluric standard star is observed close in time with the science target, photometric correction factors are on average  $\sim 10 - 15\%$ . Therefore, errors on the luminosity-based dust radius are assumed to be  $\sim 10\%$ .

## 4 Results and discussion

Based on two well-studied sources, namely, NGC 5548 and Mrk 876, Landt et al. (2023) have recently suggested that there are considerable similarities between the hot dust in AGN and that present in protoplanetary disks around young stars. In particular, these similarities are as follows: 1) the prevalence of large dust grain sizes, which, in protoplanetary disks, might have formed in the midplane of the disk by differential settling; 2) the presence of an ‘inner hole’ beyond the dust-free zone expected due to dust sublimation, which, in protoplanetary disks, is thought to be a cavity filled with gaseous disk material that can change its optical thickness and, thus, influence the location of the puffed-up so-called ‘wall’ or ‘inner rim’; and 3) a general temperature–radius relationship consistent with that for a dusty, flared, and passively illuminated protoplanetary disk. Here, we will test and expand on this proposition by using a sample of  $\sim 40$  AGN.

### 4.1 Prevalence of large grains in the hot dust of AGN

As discussed in Landt et al. (2023), the assumption of dust, which is optically thick to the UV/optical radiation heating it and optically thin to its own IR radiation, allows us to constrain the astrochemistry of the dust through the dust emissivity parameter  $Q^{\text{em}}$  (see Eq. 1) if the dust radius can be measured by an independent method. Fortunately, several such methods exist, including, e.g., the dust response time measured through reverberation mapping and a geometric dust radius measurement based on near-IR interferometry. Here, we have compiled dust radius measurements from these two independent methods for a sample of AGN with available near-IR spectra that were suitable to derive luminosity-based dust radii. Figure 1 plots the comparison between the luminosity-based dust radius and that obtained by an independent method, which was mostly near-IR photometric reverberation mapping. We note that the two dust radii are generally not contemporaneous and so could be affected by the variability effects of the irradiating luminosity, although Landt et al. (2019) argued that the hot dust radius is not set by sublimation and is probably luminosity-invariant.

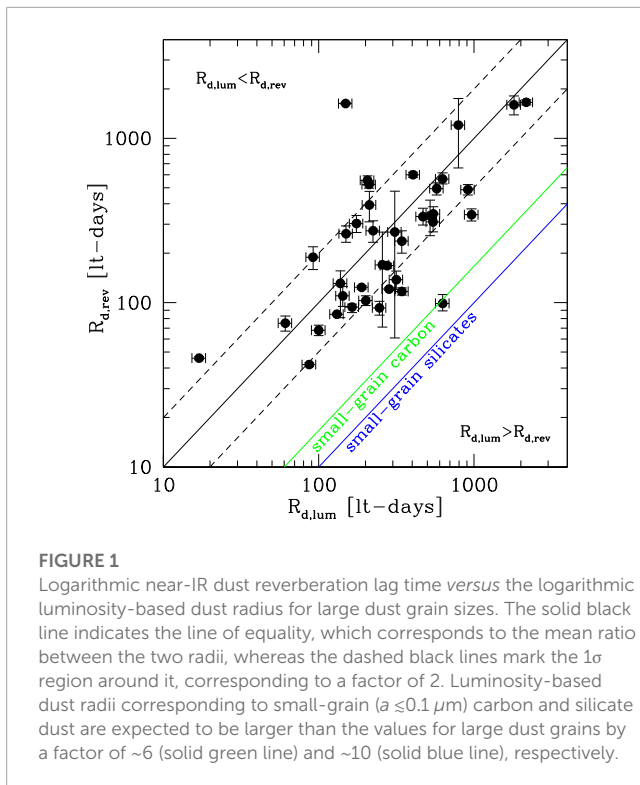


**FIGURE 1**  
Logarithmic near-IR dust reverberation lag time *versus* the logarithmic luminosity-based dust radius for large dust grain sizes. The solid black line indicates the line of equality, which corresponds to the mean ratio between the two radii, whereas the dashed black lines mark the  $1\sigma$  region around it, corresponding to a factor of 2. Luminosity-based dust radii corresponding to small-grain ( $a \leq 0.1 \mu\text{m}$ ) carbon and silicate dust are expected to be larger than the values for large dust grains by a factor of  $\sim 6$  (solid green line) and  $\sim 10$  (solid blue line), respectively.

Figure 1 shows that the large majority of the data points cluster around the line of equality for a blackbody emissivity, which corresponds to the largest dust grains. The mean ratio is  $R_{d,lum}/R_{d,rev} = 1$ , with a dispersion around the mean of a factor of  $\sim 2$ . We note that for most sources, the luminosity-based dust radius is *larger* than the dust radius measured by the independent method. Assuming instead an emissivity corresponding to small dust grains of predominantly carbonaceous or silicate composition would move the line of equality to luminosity-based dust radii larger by a factor of  $\sim 6$  (green solid line) and  $\sim 10$  (blue solid line), respectively. Although in a handful of sources this possibility cannot be excluded, in general, small grains do not seem to dominate the hot dust composition.

## 4.2 A flared, passively illuminated (hot) dusty disk with an ‘inner hole’ in AGN

It is in general of high interest to understand the origin of the scatter in Figure 1 if it is caused by AGN physics rather than being mainly due to variability and/or measurement uncertainties. Such an investigation is particularly timely since considerable research is under way to help establish the hot dust radius as a suitable standard candle for cosmological studies using AGN (e.g., Höning et al., 2017). A first indication that a considerable inconsistency can be present between the luminosity-based hot dust radius and that obtained by other means was found for the high-luminosity AGN Mrk 876 by Landt et al. (2023). The difference between the two values of a factor of  $\sim 2$  could be well explained if the dust was assembled in a flared, disk-like geometry, which is naturally expected to be carved out by the anisotropy of the accretion disk illumination (Kawaguchi and

Mori, 2010; 2011). Then, the dust is expected to be illuminated by the UV/optical accretion disk luminosity reduced by a factor  $\cos \theta$ , with  $\theta$  the angle between the accretion disk rotation axis and the location of the dust. Since such a pronounced difference was not found for the low-luminosity AGN NGC 5548 by the study of Landt et al. (2019), there is a strong possibility that the anisotropy effect depends on the AGN luminosity. An indication that the accretion disk illumination anisotropy considered by Kawaguchi and Mori (2010, 2011) affects low- and high-luminosity AGN differently was also found by Minezaki et al. (2019). Their sample showed a best-fit slope for the logarithmic reverberation dust radius *versus* optical luminosity relationship of  $\sim 0.4$ , i.e., shallower than the slope of 0.5 predicted by radiative equilibrium considerations (see Eq. 1).

Figure 2 (left panel) investigates this conjecture, where we plot the total accretion disk luminosity estimated from the fits to the near-IR spectroscopy *versus* the ratio between the luminosity-based dust radius and the dust radius measured by reverberation mapping (or near-IR interferometry). There is clearly a trend for the dust radius ratio to increase with luminosity and so for the disk structure to be more pronounced in high-luminosity sources. The significance of a linear correlation is  $p = 95.5\%$ . Figure 2 (right panel) plots the dependence of the dust radius ratio on the dust temperature. The dust temperatures reach values well above the sublimation temperature for silicates (of  $\sim 1400$  K), and therefore, the hot dust in AGN is most likely carbonaceous, as already argued previously (e.g., Mor et al., 2009; Landt et al., 2011a; Landt et al., 2019). A trend is present also in Figure 2 (right panel) that indicates that the ‘inner hole’ of the disk is more enlarged in high-luminosity sources if we assume a single chemical species for the hot dust and so a unique sublimation temperature (e.g.,  $\sim 1900$  K, corresponding to carbonaceous dust). The significance of a linear correlation is  $p = 93.5\%$ . However, we note that the scatter is considerable in both relationships shown in Figure 2.

## 4.3 Outer dusty edge of accretion disks in AGN

A considerably tighter relationship is present between the hot dust covering factor, defined as the ratio between the total dust luminosity and the total accretion disk luminosity, and the dust radius ratio (see Figure 3). The significance of a linear correlation is  $p > 99.999\%$  for a best-fit relationship of  $\log(L_d/L_{UV}) = (-0.72 \pm 0.05) - (0.84 \pm 0.15) \cdot \log(R_{d,lum}/R_{d,rev})$ . This relationship could be interpreted as evidence that the ratio between the luminosity-based dust radius and that measured by reverberation mapping (or near-IR interferometry) is a suitable indicator of the dust geometry. Then, the larger this ratio, the more pronounced the flared, dusty disk structure and so the lower the expected dust covering factor. In other words, as the ratio increases, the dust geometry moves from almost circular to a short disk component with a large flare and eventually to a long disk component with a smaller flare. A sketch of this possible change in dust geometry is shown in Figure 4. Baskin and Laor (2018) investigated the geometry of a dusty, inflated accretion disk structure. Although they assumed largely varying grain sizes (spanning about two orders of magnitude), which resulted in the

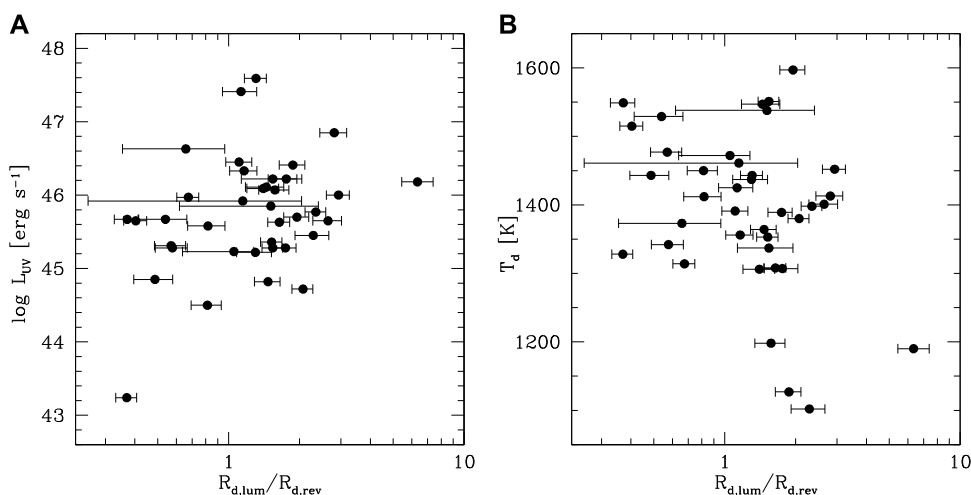


**FIGURE 2** Logarithmic total accretion disk luminosity (A) and the dust temperature (B) versus the logarithm of the ratio between the luminosity-based dust radius and the dust radius measured by reverberation mapping (or near-IR interferometry).

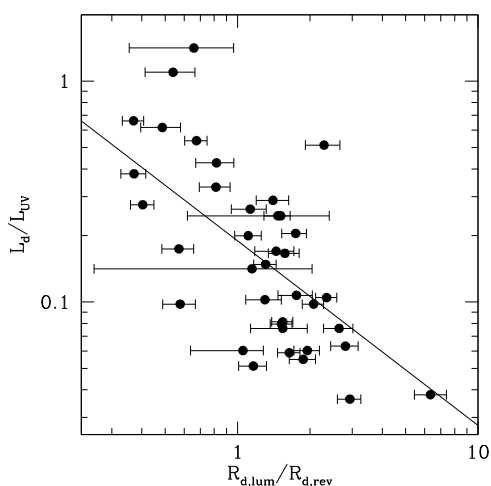


**FIGURE 3** Logarithmic hot dust covering factor versus the logarithm of the ratio between the luminosity-based dust radius and the dust radius measured by reverberation mapping (or near-IR interferometry). The best-fit relationship is shown as the black solid line. See text for more details.

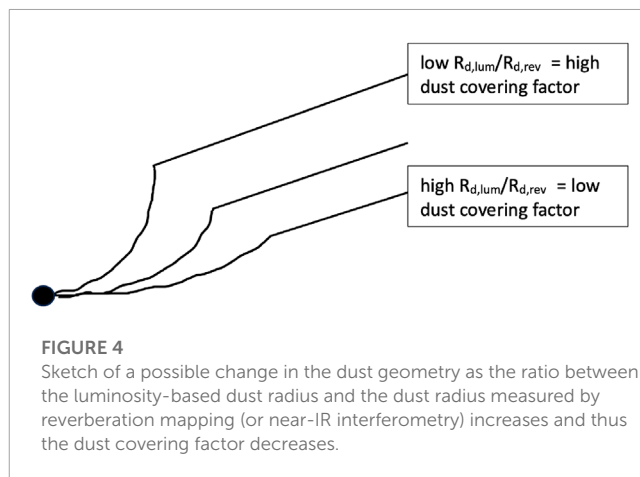


**FIGURE 4** Sketch of a possible change in the dust geometry as the ratio between the luminosity-based dust radius and the dust radius measured by reverberation mapping (or near-IR interferometry) increases and thus the dust covering factor decreases.

sublimation process occurring over a transition zone rather than at a single location, the scale height of this geometry could be related to the change in dust geometry proposed here. In their model, the disk height is set by the balance between the effects of gravity and radiation pressure, and depends only on the accretion rate and the opacity of the material (see their eq. 22). Therefore, it predicts that more luminous AGN have higher dust covering factors, which is contrary to the observed relationship presented in Figure 2.

Recently, Landt et al. (2023) presented the comparison of the mean and variable (rms) spectrum in the high-luminosity AGN Mrk

876, which showed clearly that at least two hot dust components are present in AGN. They found that the total dust emission was dominated (at the ~70% level) by the non-variable component, which could have its origin in the outer (flared) part of the dusty disk or the outer dusty edge of the accretion disk or both. How would such a second hot dust component manifest itself in the relationship shown in Figure 3? We would need to know the viewing angle,  $\theta$ , in order to estimate the accretion disk luminosity as seen by the dust. Then, the true dust covering factor should be calculated relative to this (reduced)  $L_{UV}$ . In other words, if the main origin of the second dust component is from the flare, the more correct our already assumed accretion disk luminosity is. However, if the main origin of the second dust component is instead in the accretion disk, we should expect to have *overestimated* the accretion disk luminosity as seen by the dust and, therefore, *underestimated* the dust covering factor. If indeed the dust radius ratio is a suitable indicator of the dust geometry as described previously, as this value increases, the flare becomes less important and the accretion disk

dust more important, thus apparently reducing the dust covering factor and tightening the relationship displayed in Figure 3. We note that although the dust in the accretion disk will not necessarily be externally illuminated, if it is composed of  $\mu\text{m}$ -sized grains, it will be well-coupled to the accretion disk gas and so affected by its (transmitted) total luminosity in a similar way. Stalevski et al. (2016) investigated in detail the effects of the anisotropy of the accretion disk luminosity on the covering factor for the torus dust. They found that for type 1 AGN, low and high covering factors will be underestimated and overestimated, respectively, with the effect being more pronounced for the former than for the latter (see their Fig. 10). Their results could partly explain the steep slope we find for the relationship in Figure 3 and also the fact that we find dust covering factors exceed unity and extremely low values (of only a few per cent).

## 5 Conclusion

This study used a sample of  $\sim 40$  AGN with available cross-dispersed near-IR spectroscopy to perform a comparison between luminosity-based dust radii and those obtained by independent methods, e.g., by reverberation mapping. The main aim was to reveal the astrochemistry and geometry of the hot dust in AGN. The main results can be summarized as follows:

- 1) It could be shown that luminosity-based dust radii obtained with the assumption of a blackbody emissivity were consistent within a factor of  $\sim 2$  with dust radii obtained by independent methods. Therefore, large dust grains (with sizes of a few  $\mu\text{m}$ ) appear to be ubiquitous in the hot dust of AGN. Assuming instead an emissivity corresponding to small dust grains implied much larger luminosity-based dust radii (by factors of  $\sim 6 - 10$ ).
- 2) We found a tight relationship between the dust covering factor and the ratio between the luminosity-based dust radius and the dust radius measured by reverberation mapping (or near-IR interferometry). This new relationship can be understood if one assumes that the dust radius ratio is a suitable indicator of the dust geometry and that hot dust is present in the accretion disk in addition to that assembled in a flared, dusty disk, as proposed by Landt et al. (2023).
- 3) The effects of the anisotropy of the accretion disk illumination might be different for low- and high-luminosity AGN, as

suggested by the flattening of the slope at high luminosities in the dust radius-luminosity plane of Minezaki et al. (2019). We find a trend that the dust radius ratio increases with AGN luminosity, indicating a change in dust geometry whereby the disk structure becomes more pronounced in the high-luminosity AGN.

## Data availability statement

The raw data supporting the conclusion of this article will be made available by the authors, without undue reservation.

## Author contributions

HL: data curation, formal analysis, and writing-original draft.

## Acknowledgments

HL acknowledges a Daphne Jackson Fellowship sponsored by the Science and Technology Facilities Council (STFC), United Kingdom, and support from STFC grants (ST/P000541/1, ST/T000244/1, and ST/X001075/1).

## Conflict of interest

The author declares that the research was conducted in the absence of any commercial or financial relationships that could be construed as a potential conflict of interest.

## Publisher's note

All claims expressed in this article are solely those of the authors and do not necessarily represent those of their affiliated organizations, or those of the publisher, the editors, and the reviewers. Any product that may be evaluated in this article, or claim that may be made by its manufacturer, is not guaranteed or endorsed by the publisher.

## References

- Amorim, A., Bourdarot, G., Brandner, W., Cao, Y., Clénet, Y., Davies, R., et al. (2023). Toward measuring supermassive black hole masses with interferometric observations of the dust continuum. *A&A* 669, A14. doi:10.1051/0004-6361/202244655
- Baskin, A., and Laor, A. (2018). Dust inflated accretion disc as the origin of the broad line region in active galactic nuclei. *MNRAS* 474, 1970–1994. doi:10.1093/mnras/stx2850
- Bentz, M. C., and Katz, S. (2015). The AGN black hole mass database. *PASP* 127, 67–73. doi:10.1086/679601
- Clavel, J., Wamsteker, W., and Glass, I. S. (1989). Hot dust on the outskirts of the broad-line region in Fairall 9. *ApJ* 337, 236–250. doi:10.1086/167100
- Czerny, B., Li, Y.-R., Hryniewicz, K., Panda, S., Wildy, C., Sniegowska, M., et al. (2017). Failed radiatively accelerated dusty outflow model of the broad line region in active galactic nuclei. I. Analytical solution. *ApJ* 846, 154. doi:10.3847/1538-4357/aa8810
- Dexter, J., Shangquan, J., Hönig, S., Kishimoto, M., Lutz, D., Davies, R., et al. (2020). The resolved size and structure of hot dust in the immediate vicinity of AGN. *A&A* 635, A92. doi:10.1051/0004-6361/201936767
- García-Rissmann, A., Rodríguez-Ardila, A., Sigut, T. A. A., and Pradhan, A. K. (2012). A near-infrared template derived from I zw 1 for the Fe II emission in active galaxies. *ApJ* 751, 7. doi:10.1088/0004-637X/751/1/7
- Glass, I. S. (2004). Long-term infrared photometry of Seyferts. *MNRAS* 350, 1049–1066. doi:10.1111/j.1365-2966.2004.07712.x
- Hönig, S. F., Watson, D., Kishimoto, M., Gandhi, P., Goad, M., Horne, K., et al. (2017). Cosmology with AGN dust time lags-simulating the new VEILS survey. *MNRAS* 464, 1693–1703. doi:10.1093/mnras/stw2484
- Kawaguchi, T., and Mori, M. (2011). Near-infrared reverberation by dusty clumpy tori in active galactic nuclei. *ApJ* 737, 105. doi:10.1088/0004-637X/737/2/105

- Kawaguchi, T., and Mori, M. (2010). Orientation effects on the inner region of dusty torus of active galactic nuclei. *ApJL* 724, L183–L187. doi:10.1088/2041-8205/724/2/L183
- Kishimoto, M., Hönig, S. F., Antonucci, R., Kotani, T., Barvainis, R., Tristram, K. R. W., et al. (2009). Exploring the inner region of type 1 AGNs with the Keck interferometer. *A&A* 507, L57–L60. doi:10.1051/0004-6361/200913512
- Koshida, S., Minezaki, T., Yoshii, Y., Kobayashi, Y., Sakata, Y., Sugawara, S., et al. (2014). Reverberation measurements of the inner radius of the dust torus in 17 seyfert galaxies. *ApJ* 788, 159. doi:10.1088/0004-637X/788/2/159
- Krolik, J. H. (2007). AGN obscuring tori supported by infrared radiation pressure. *ApJ* 661, 52–59. doi:10.1086/515432
- Landt, H., Bentz, M. C., Peterson, B. M., Elvis, M., Ward, M. J., Korista, K. T., et al. (2011a). The near-infrared radius-luminosity relationship for active galactic nuclei. *MNRAS* 413, L106–L109. doi:10.1111/j.1745-3933.2011.01047.x
- Landt, H., Bentz, M. C., Ward, M. J., Elvis, M., Peterson, B. M., Korista, K. T., et al. (2008). The near-infrared broad emission line region of active galactic nuclei. I. the observations. *ApJS* 174, 282–312. doi:10.1086/522373
- Landt, H., Elvis, M., Ward, M. J., Bentz, M. C., Korista, K. T., and Karovska, M. (2011b). The near-infrared broad emission line region of active galactic nuclei. II. the 1- $\mu$ m continuum. *MNRAS* 414, 218–240. doi:10.1111/j.1365-2966.2011.18383.x
- Landt, H., Mitchell, J. A. J., Ward, M. J., Mercatoris, P., Pott, J.-U., Horne, K., et al. (2023). A complex dust morphology in the high-luminosity AGN Mrk 876. *ApJ* 945, 62. doi:10.3847/1538-4357/acb92d
- Landt, H., Ward, M. J., Elvis, M., and Karovska, M. (2014). Constraints on the outer radius of the broad emission line region of active galactic nuclei. *MNRAS* 439, 1051–1062. doi:10.1093/mnras/stu031
- Landt, H., Ward, M. J., Kynoch, D., Packham, C., Ferland, G. J., Lawrence, A., et al. (2019). The first spectroscopic dust reverberation programme on active galactic nuclei: the torus in NGC 5548. *MNRAS* 489, 1572–1589. doi:10.1093/mnras/stz2212
- Landt, H., Ward, M. J., Peterson, B. M., Bentz, M. C., Elvis, M., Korista, K. T., et al. (2013). A near-infrared relationship for estimating black hole masses in active galactic nuclei. *MNRAS* 432, 113–126. doi:10.1093/mnras/stt421
- Lyu, J., Rieke, G. H., and Smith, P. S. (2019). Mid-IR variability and dust reverberation mapping of low- $z$  Quasars. I. Data, methods, and basic results. *ApJ* 886, 33. doi:10.3847/1538-4357/ab481d
- Minezaki, T., Yoshii, Y., Kobayashi, Y., Sugawara, S., Sakata, Y., Enya, K., et al. (2019). Reverberation measurements of the inner radii of the dust tori in Quasars. *ApJ* 886, 150. doi:10.3847/1538-4357/ab4f7b
- Monnier, J. D., Millan-Gabet, R., Billmeier, R., Akeson, R. L., Wallace, D., Berger, J. P., et al. (2005). The near-infrared size-luminosity relations for herbig ae/Be disks. *ApJ* 624, 832–840. doi:10.1086/429266
- Mor, R., Netzer, H., and Elitzur, M. (2009). Dusty structure around type-I active galactic nuclei: clumpy torus narrow-line region and near-nucleus hot dust. *ApJ* 705, 298–313. doi:10.1088/0004-637X/705/1/298
- Phinney, E. S. (1989). “Dusty disks and the infrared emission from AGN;” *Theory of accretion disks*. Editor F. Meyer (of NATO Advanced Study Institute ASI Series C), 290, 457.
- Prieto, A., Rodríguez-Ardila, A., Panda, S., and Marinello, M. (2022). A novel black hole mass scaling relation based on coronal gas, and its dependence with the accretion disc. *MNRAS* 510, 1010–1030. doi:10.1093/mnras/stab3414
- Ramolla, M., Haas, M., Westhues, C., Pozo Nuñez, F., Sobrino Figaredo, C., Blex, J., et al. (2018). Simultaneous H $\alpha$  and dust reverberation mapping of 3C 120: testing the bowl-shaped torus geometry. *A&A* 620, A137. doi:10.1051/0004-6361/201732081
- Riffel, R., Rodríguez-Ardila, A., and Pastoriza, M. G. (2006). A 0.8–2.4  $\mu$ m spectral atlas of active galactic nuclei. *A&A* 457, 61–70. doi:10.1051/0004-6361:20065291
- Salpeter, E. E. (1977). Formation and destruction of dust grains. *ARA&A* 15, 267–293. doi:10.1146/annurev.aa.15.090177.001411
- Schnülle, K., Pott, J.-U., Rix, H.-W., Decarli, R., Peterson, B. M., and Vacca, W. (2013). Dust physics in the nucleus of NGC 4151. *A&A* 557, L13. doi:10.1051/0004-6361/201321802
- Schnülle, K., Pott, J.-U., Rix, H.-W., Peterson, B. M., De Rosa, G., and Shappee, B. (2015). Monitoring the temperature and reverberation delay of the circumnuclear hot dust in NGC 4151. *A&A* 578, A57. doi:10.1051/0004-6361/201525733
- Shablovinskaya, E. S., Afanasiev, V. L., and Popović, L. č. (2020). Measuring the AGN sublimation radius with a new approach: reverberation mapping of broad line polarization. *ApJ* 892, 118. doi:10.3847/1538-4357/ab7849
- Stalevski, M., Ricci, C., Ueda, Y., Lira, P., Fritz, J., and Baes, M. (2016). The dust covering factor in active galactic nuclei. *MNRAS* 458, 2288–2302. doi:10.1093/mnras/stw444